Computers and Concrete, *Vol. 20, No. 1 (2017) 99-110*
DOI: https://doi.org/10.12989/cac.2017.20.1.099

Concrete structures under combined mechanical and environmental actions: Modelling of durability and reliability

Dita Vořechovská[*1], Martina Šomodíková[1a], Jan Podroužek[1a], David Lehký[1b] and Břetislav Teplý[2c]

[1]*Institute of Structural Mechanics, Faculty of Civil Engineering, Brno University of Technology, Veveří 331/95, 602 00 Brno, Czech Republic*
[2]*Institute of Chemistry, Faculty of Civil Engineering, Brno University of Technology, Veveří 331/95, 602 00 Brno, Czech Republic*

(Received January 1, 2016, Revised March 10, 2017, Accepted March 25, 2017)

Abstract. Service life assessments which do not include the synergy between mechanical and environmental loading are neglecting a factor that can have a significant impact on structural safety and durability assessment. The degradation of concrete structure is a result of the combined effect of environmental and mechanical factors. In order to make service life design realistic it is necessary to consider both of these factors acting simultaneously. This paper deals with the advanced modelling of concrete carbonation and chloride ingress into concrete using stochastic 1D and 2D models. Widely accepted models incorporated into the new fib Model Code 2010 are extended to include factors that reflect the coupled effects of mechanical and environmental loads on the durability and reliability of reinforced concrete structures. An example of cooling tower degradation by carbonation and an example of a bended reinforced concrete beam kept for several years in salt fog are numerically studied to show the capability of the stochastic approach. The modelled degradation measures are compared with experimental results, leading to good agreement.

Keywords: concrete structures; synergy; mechanical loading; environmental loading; modelling; service life; reliability

1. Introduction

Infrastructure performance, namely the durability of concrete structures and appropriate reliability, is influenced by several forms of attack, such as chemical attack (e.g., concrete carbonation, chloride ingress, acid attack and others), electrochemical attack (corrosion of reinforcement), physical attack (e.g., freeze/thaw), and mechanical load (static or dynamic). In the prevailing number of cases the assessments for different forms of attack are treated separately. However, general service life assessments or predictions which do not include the synergy of mechanical and environmental load are neglecting a factor that can have a significant impact on structural safety and durability prognosis (RILEM 2013, Tang *et al.* 2015). In order to make service life design realistic it is necessary to take into consideration both mechanical and environmental loads acting simultaneously. Due to the actual stress and/or deformation field, some significant changes in pore structure and crack formation may be recorded. Moreover, damage due to corrosion of reinforcement is recognized as one of the major causes of the deterioration of reinforced concrete structures; in the presence of defects, a high corrosion rate might be promoted even at a low water-cement ratio (Miyazato and Otsuki 2010).

∗Corresponding author, Ph.D.
E-mail: vorechovska.d@fce.vutbr.cz
[a]Ph.D.
[b]Associate Professor
[c]Professor

Due to the huge number of possible stress configurations governed by structure and load types, their investigation via experimental techniques is not feasible and so the usefulness of modelling is clearly apparent. The significance of reliable and approved models is also stressed by the new Model Code 2010 by *fib* (2012), where the probabilistic safety format is presented, and the utilization of mathematical models and the enhancement of the design of structures for durability are advocated. Due to inherent uncertainties in material, technological and environmental characteristics, stochastic models are used, thus creating an effective tool for the assessment and prediction of time-dependent degradation processes. The involved uncertainties (both epistemic and aleatory) need to be given proper consideration. However, it should be noted that the utilization of models may sometimes introduce problems as there is no consensus on the most appropriate degradation models to be employed, the requirement for the acceptable probability of reaching the relevant limit state, or the values and statistical characterization of the input parameters. To prevent the predisposition of a probabilistic approach to the manipulation of the input, it is believed that sensitivity analysis is a useful tool which can significantly help in avoiding this negative aspect of such an approach. Furthermore, the performance-based approach (Beuhausen 2014) may be supported by the employment of modelling. The basic principles and software implementation of assessing and updating the reliability of concrete bridges subjected to spatial deterioration and the utilization of inspection and monitoring information has been recently presented by Schneider *et al.* (2015).

In the presented contribution, an effective approach for the assessment and prediction of time-dependent

http://www.techno-press.org/?journal=cac&subpage=8
ISSN: 1598-8198 (Print), 1598-818X (Online)

degradation processes with stochastic models that consider the simultaneous effect of concrete carbonation or chloride penetration and mechanical load will be introduced. FReET-D software, an efficient tool for statistical, sensitivity and reliability analyses (Novák *et al.* 2014) for use in degradation modelling, is therefore supplemented by several analytical 1D models which consider the uncertainties of the involved variables. Employing statistical processing, the reliability level can be assessed based on a relevant limit state, and a service life prognosis can be made. To enable 2D modelling, the Cellular Automata technique has been employed as well. The results presented here thus reflect the coupled effects of mechanical and environmental loads on durability and the relevant reliability of reinforced concrete structures.

To partially verify the proposed methodology, examples of carbonation and chloride ingress are proposed and discussed in this paper. First, the degradation of a cooling tower due to carbonation is numerically studied. The modelled degradation effects have been compared with experimental results in this case. Second, experimental measurements performed on reinforced concrete beams loaded in three point flexion and placed in a chloride environment are compared to numerical simulations. Moreover, to show the capability of the stochastic approach, parametric studies using models which couple the effects of carbonation or chloride ions and mechanical loading are presented.

2. Service life format

Verification of limit states associated with the durability of structures may be performed according to Model Code 2010 (*fib* 2012) using different approaches; note that only the fully probabilistic approach provides quantitative information about safety level. It appears that predictive models are needed to estimate how the resistance, loads and safety level of concrete structures undergoing deterioration will change over time.

In the case of durability, the service life format involves determining the remaining design life, t_D, of a structure or structural component and its comparison with the predicted service life, t_S. In order to ensure the safety of the structure and its components, their predicted service lives, t_S, should meet or exceed their design lives, t_D, i.e.,

$$t_S \geq t_D \tag{1}$$

The probability of failure, P_f, at time t_D is compared with the specific target probability value, P_d

$$P_f(t_D) = \mathrm{P}\{t_S \leq t_D\} \leq P_d \tag{2}$$

The service life t_S can be determined as the sum of two service life predictors (periods)

$$t_S = t_i + t_p \tag{3}$$

where t_i is the time at which the initiation of reinforcement corrosion takes place (so-called initiation time) and t_p is the part of the design life after corrosion initiation (the propagation period). Frequently, the initiation period only serves as a decisive limit state considered to be a limit for service life with a good safety margin, i.e.,

$$t_s = t_i \tag{4}$$

As an alternative to Eq. (2) for failure probability assessment the general form can be used

$$P_f(t_D) = \mathrm{P}\{B(t_D) - A(t_D) \leq 0\} \leq P_d \tag{5}$$

where A is the action effect and B is the barrier at time t_D. In the case of carbonation, B is represented by concrete cover a and A is represented by x_c – the depth of carbonation at time t_D.

When the effects of chloride ion ingress are dealt with, the barrier $B = C_{cr}$ is the critical concentration of dissolved Cl^- (a prerequisite of steel depassivation) and $A = C_a$ is the concentration of Cl^- at the reinforcement at time t_D.

Note the reliability level can also be expressed by the reliability index β in practice. This indicator of structural reliability is well-known today and is prescribed in design codes. In the case of the service life format the value β is then compared with the target reliability level defined by the design value of the reliability index, β_d.

3. Concrete structures under the combined actions of mechanical and environmental load

3.1 Mechanical load effects

Due to the natural spread of environmental, material and load characteristics it is important for proper stochastic modelling of structural deterioration to take into account the variability of decisive parameters; primarily material and load characteristics play the most important role. Particularly the loading of a structure causes the stress field within the structure vary, and the related spatial crack distribution subsequently affects the rate of structural deterioration. With regard to crack distribution, possible corrosion initiation and propagation in reinforced concrete structures show spatial fluctuations which could significantly influence the structural and serviceability performance of structural systems as well as structural reliability.

To assess the stress field, a nonlinear analysis of the structural response, reliability and durability of concrete structures can be performed in practice using finite element method computational models and advanced material models based on fracture and damage mechanics. Such models are able to realistically predict and assess the allowable loading conditions for ultimate as well as serviceability limit states.

In order to model the spatial variability of degradation, random fields utilized within the framework of stochastic finite element methods can be employed. The method based on the orthogonal transformation of a covariance matrix for random field simulation (Vanmarcke *et al.* 1986) can be efficiently used. However, the sample size reduction technique for such a Monte Carlo (MC) simulation task is yet to be formulated. A contribution to sampling scenarios involving spatial variability was recently presented by

Podroužek *et al.* (2014, 2015).

In the case of input scalar random variables, the MC task can be effectively reduced by utilizing the stratified simulation technique Latin Hypercube Sampling (Mckay *et al*. 1979). The result of this combination is that only a few random variables and quite a small number of simulations are necessary for accurate representation compared to the classical MC simulation method. These findings are also employed in (Novák *et al.* 2014) and in subsequent parts of the present paper.

3.2 Concrete carbonation and mechanical load

Pore distribution and size can be modified considerably by the action of applied mechanical load as well as by the opening and/or closing of microcracks and the formation of new cracks. The influence of these effects on carbonation progress has recently been proved experimentally – see the annotated bibliography (RILEM 2013, Wittmann *et al.* 2012). A relatively low compressive load decreases the rate of carbonation due to the partial closing of microcracks under applied compressive stress. Loading which increases above 50% of the ultimate load results in the ongoing closure of microcracks while the formation of new cracks is in progress with an effect on permeability and carbonation rate, which both increase. Also, the tensile stress opens new microcracks and therefore the rate of carbonation increases steadily with increasing applied load.

Generally, the carbonation depth, x_c, over time, t, without consideration of mechanical load, can be approximated simply as a product of the constant and square root of time. The constant A accounts for concrete mix, type of cement, the ambient relative humidity, CO_2 content in the atmosphere, curing conditions and other parameters. Any suitable carbonation model may be utilized for the determination of A.

To take into consideration the impact of an applied stress σ due to mechanical load on carbonation progress, a correction factor, k_σ, is introduced (Wittmann *et al.* 2012). It is determined on the basis of results obtained from four point bending test series (accelerated carbonation) performed on two types of concrete mix. Any carbonation model can be extended simply by the factor k_σ and then the carbonation depth over time is defined as

$$x_c(t) = k_\sigma A\sqrt{t} \tag{6}$$

Different equations are valid to assess the correction factor k_σ for parts of the concrete structure where the tensile stresses, σ_t, or compressive stresses, σ_c, are being considered. The correction factor is defined for concrete under tensile load and compressive load, respectively, as

$$k_\sigma\left(\sigma_t/\sigma_{u,t}\right) = 1 + 1.41\left(\sigma_t/\sigma_{u,t}\right) + 0.82\left(\sigma_t/\sigma_{u,t}\right)^2 \quad \text{and} \tag{7}$$

$$k_\sigma\left(\sigma_c/\sigma_{u,c}\right) = 1 - 2.27\left(\sigma_c/\sigma_{u,c}\right) + 4.86\left(\sigma_c/\sigma_{u,c}\right)^2 \tag{8}$$

respectively, where $\sigma_{u,t}$ and $\sigma_{u,c}$ represent the ultimate strength in tension and ultimate strength in compression, respectively. As an option for Eqs. (7)–(8), the factor k_σ is considered to be a random quantity given by the user. In this way the involved uncertainties or partial lack of knowledge can be reflected as well as possible results of other experiments.

For the sake of completeness, some other synergy effects may be treated similarly by the use of a different correction factor (e.g., the influence of cyclic load on concrete porosity and the consequent rate of concrete carbonation, the influence of frost action on carbonation and chloride penetration, or how carbonation may facilitate chloride penetration). However, the proper values of these factors have not been specified yet (to the authors' best knowledge).

In the case of carbonation, the general limit Eq. (5) can be specialized into the following form

$$P_f(t_D) = \mathrm{P}\{a - x_c(t_D) \le 0\} \le P_d \tag{9}$$

which means that the reinforcement depassivation and consequent corrosion of reinforcement initiates at a time when the carbonation depth, x_c, permeates through the whole thickness of concrete cover, a. A conservative estimate of the service life is made based on Eq. (9), and the reliability level over time can also be predicted.

3.3 Chloride ingress and mechanical load

Chloride ions are also able to damage the passivating layer on reinforcing bars and trigger steel corrosion; in order to predict the durability performance of RC structures it is necessary to study chloride penetration, which is a complex process. Transport characteristics in concrete may vary significantly depending on concrete composition, materials, curing, age, and environmental conditions, and also on its current pore and/or crack structure (RILEM 2013, *fib* 2012). Chlorides penetrating into concrete may be transported by diffusion and capillary suction. Moreover, the external chloride concentration can vary over space and time, and some chloride ions become immobile (bounded) due to chemical reactions or physical adsorption. So, the total concentration of chloride ions C_t is the sum of free ion concentration C_f (ions dissolved in the pore water) and the concentration of bound ions C_b. Only the free ions take part in the diffusion process and are able to cause the depassivation of steel reinforcement (*fib* 2012, Yuan *et al.* 2009).

Often, the simplified model for chloride ingress is adopted, based on Fick's 2nd law with consideration given to the "convection zone" (*fib* 2006), which is the most external concrete layer of thickness Δx where the behaviour of chlorides entering the concrete is not subject to a diffusion process. The maximum concentration of Cl^- is produced at the position $x = \Delta x$, which is often reported from about 0.5 to 20 mm. The diffusion process is then applied starting at depth Δx.

In uncracked concrete the closed-form solution of the governing equation for the 1D problem (assuming a semi-infinite body of saturated concrete) reads for chloride concentration C (*fib* 2006), neglecting the initial chloride content in concrete

$$C(x - \Delta x, t) = C_{S,\Delta x}\left(1 - \mathrm{erf}\,\frac{x - \Delta x}{\sqrt{t \cdot D_{app,C}}}\right) \tag{10}$$

where $C_{S,\Delta x}$ is the chloride content at depth Δx and at a certain point of time t (wt.-%/c) (a substitute for the surface content of chloride); $D_{\mathrm{app,C}}$ is the apparent coefficient of chloride diffusion (mm^2/years) and *erf* is the error function

$$\operatorname{erf}\left(z\right)=\frac{2}{\sqrt{\pi}}\int_0^z \exp\left(-t^2\right)\,\mathrm{d}t \qquad (11)$$

The value of $D_{\mathrm{app,C}}$ decreases with time depending, among other things, on cement/binder type and amount, water/binder ratio, and temperature, and is subject to considerable scatter. According to *fib* (2006), $D_{\mathrm{app,C}}$ can be determined either by use of the "chloride profiling method" (the profiles being taken from existing structure samples; for the design of new structures from test samples stored under conditions similar to those expected in the real world), which is rather time consuming, or, as a second option, by the empirically derived approach shown in (*fib* 2006), i.e., by means of the equation

$$D_{\mathrm{app,C}}=k_{\mathrm{e}}D_{\mathrm{RCM,0}}\left(\frac{t_0}{t}\right)^a \qquad (12)$$

where $D_{\mathrm{RCM,0}}$ is the chloride migration coefficient (mm^2/years), k_{e} is the environmental transfer variable (considering temperature), t_0 is the reference point in time (usually 28 days = 0.0767 years), t is time (years) and a is the ageing exponent. A detailed description of the individual quantities is given in (*fib* 2006), Annex B, and it is not repeated in the present text; note that the influence of time, chloride ion bounding, concrete composition and environmental conditions are considered directly or indirectly within this approach. To obtain and quantify reliable data for such an approach is not an easy task (Lollini *et al.* 2015).

A different strategy is therefore also described by other researchers – see (Fu *et al.* 2015, Zhang *et al.* 2011, Oh and Jang 2007) – in which the chloride diffusivity is modelled by means of influencing factors as follows

$$D_{\mathrm{app,C}}=D_{\mathrm{app,C,ref}}F_{\mathrm{b}}F_{\mathrm{T}}F_{\mathrm{t}}F_{\mathrm{h}}F_{\mathrm{w}}F_{\varepsilon}F_{\mathrm{c}}F_{\mathrm{e}} \qquad (13)$$

where $D_{\mathrm{app,C,ref}}$ is the reference chloride diffusivity, e.g., the diffusivity in saturated concrete made from OPC, at the age of 28 days. F_{b} is the chloride binding effect factor, which depends mainly on concrete supplementary cementitious materials which can be calculated using the corresponding binding capacity and either the linear or Langmuir isotherm (Yuan *et al.* 2009, Martín-Pérez *et al.* 2000). In (Ishida *et al.* 2009) the factor is formulated for OPC, fly ash and blast furnace slag, based on experimental data. The factor F_{T} accounts for the effect of ambient temperature, which is described e.g., in (Fu *et al.* 2015, Zhang *et al.* 2011, Oh and Jang 2007). Factor F_{t} accounts for the ageing effect (Fu *et al.* 2015, Zhang *et al.* 2011, Lollini *et al.* 2015) and F_{h} for the effect of relative humidity – see (Zhang *et al.* 2011, Oh and Jang 2007). Factor F_{c} takes into account the effect of curing conditions and recommends for curing times of 1, 3, 7 and 28 days the values 2.1, 1.5, 1.0 and 0.79, respectively (Zhang *et al.* 2011). Factor F_{e} is an environmental coefficient and values recommended for a marine environment are shown in (Zhang *et al.* 2011) for OPC concrete or concrete made with the addition of slag.

For cases of the combination of chloride penetration and mechanical load, a diffusion coefficient modified by factors F_{ε} and F_{w} is used, influenced by stress/strain state and crack formation; the diffusion coefficient depends on the pore space, the structure of the cracks and the degree of saturation. In the annotated bibliography (RILEM 2013) it is reported that pore space is modified by the application of load, while capillary absorption decreases under compressive load. Chloride diffusion slows down under moderate compressive load but increases if the applied load approaches the ultimate load. Under tensile load, both the capillary absorption and the diffusion coefficient increase steadily with increasing applied load. The diffusion coefficient can also be increased by cyclic loading.

The effect of cracking on concrete diffusivity is discussed by many researchers, e.g., in (Ishida *et al.* 2009, Wittmann *et al.* 2012, Papakonstantinou and Shinozuka 2013, Lu *et al.* 2011, Audenauert *et al.* 2009, Mu *et al.* 2013, Lu *et al.* 2014, Wang and Ueda 2011, Djerbi *et al.* 2008). The majority of these sources concentrate on the effect of a single crack only; a 2D solution is modelled by the finite element method (FEM) in (Leung and Hou 2013, Bentz *et al.* 2013, Jin *et al.* 2010). In (Papakonstantinou and Shinozuka 2013) a stochastic approach is employed, concentrating more on the propagation period, i.e., on the impact of reinforcement corrosion. In this paper an approach combining spatial variability due to both mechanical and chemical action will be demonstrated not only via a 1D solution, but also in a 2D Cellular Automata (CA) analysis of a concrete beam.

The effect of stress due to mechanical loading (stress levels preceding crack appearance, i.e., factor F_{ε}) is dealt with in (Kim *et al.* 2010, Wan *et al.* 2013). E.g., for tensile stress-strength ratios of 30% and 60%, decreases in chloride diffusivity of 11% and 29%, respectively, were detected for concretes made from OPC in (Deung *et al.* 2013).

In order to reflect the influence of load-induced cracks, utilizing factor F_{w}, the approach presented in (Zhang *et al.* 2011, Lu *et al.* 2011) is employed: for concrete with transverse load-induced cracks the average diffusion coefficient is divided into two parts for sound and cracked concrete. Thus, the factor F_{w} for such a "smeared" crack approach may be formulated as

$$F_{\mathrm{w}}=1-\frac{w}{s_{\mathrm{r,max}}}\left(1+\frac{D_{\mathrm{C}}}{D_{\mathrm{app,C,ref}}}\right) \qquad (14)$$

where w is the crack width induced by the service load, $s_{\mathrm{r,max}}$ is the maximum crack spacing and D_{C} stands for the value of the chloride diffusion coefficient inside the crack, dependent on the crack width (i.e., on the depth as well). Coefficient D_{C} (m^2/s) can be computed in a simplified way, e.g., by Djerbi *et al.* (2008)

$$D_C=\begin{cases}0 \text{ for } w<30\ \mu\mathrm{m}\\ \left(0.16w-3\right)\times10^{-10} \text{ for } 30\ \mu\mathrm{m}\le w\le 100\ \mu\mathrm{m}\\ 13\times10^{-10} \text{ for } w>100\ \mu\mathrm{m}\end{cases} \qquad (15)$$

Strictly speaking, due to the wedge shape of bending cracks their widths are not constant and the D_C value is dependent on the distance from the surface, i.e., for a certain value of x where $w \leq 30$ μm it holds that $D_C = 0$. Values can be gained for w and $s_{r,max}$ by performing measurements on an existing structure, or by FEM modelling, or by following the recommendations prescribed in (*fib* 2012, EN 1992-1-1 2004).

Note that in Eq. (13) some factors may be omitted according to the given design or assessment situation and the availability of relevant data.

Considering initiation period assessment, the limiting Eq. (5) for the case of chloride ion ingress transforms into the form

$$P_f(t_D) = P\{C_{cr} - C_a(t_D) \leq 0\} \leq P_d \tag{16}$$

where C_{cr} is the critical concentration of dissolved Cl^- leading to steel depassivation and C_a is the concentration of Cl^- at the reinforcement at time t_D.

4. Practical example for carbonation – cooling tower

The aim of this example is to present the utilization of the probabilistic modelling of degradation process prognosis, namely the carbonation of concrete. This example follows on from the results of Teplý *et al.* (2012), where the carbonation depth on a reinforced concrete cooling tower was analyzed using four different models included in FReET-D software (Novák *et al.* 2014). In this contribution, the complex model for modelling concrete carbonation is extended by a correction factor according to Eqs. (7)–(8) (Wittmann *et al.* 2012) to reflect the coupling effects of mechanical and environmental loads on the durability and reliability of reinforced concrete structures.

The cooling tower, which has a height of 206 m (built in the early seventies, w/c = 0.55, OPC, mean compressive strength measured on-site: 34 MPa), was investigated at the age of 19.1 years and the depth of carbonation was measured using phenolphthalein tests at 75 locations on both the internal and external surfaces of the shell. The measured values were averaged and therefore the spatial variability was not taken into account. At the same time, the range of reinforcement corrosion was visually observed and sorted into three classes (Keršner *et al.* 1996). In this way, relatively reliable in situ statistical data were obtained.

The process of concrete carbonation was modelled using a widely agreed model developed within European joint research and incorporated into the Model Code 2010 (*fib* 2012). The carbonation depth is defined according to the formula

$$x_c(t) = \psi \cdot \sqrt{2 \cdot k_e \cdot k_c \cdot \left(k_t \cdot R_{ACC,0}^{-1} + \varepsilon_t\right) \cdot C_S} \cdot W(t) \cdot \sqrt{t} \tag{17}$$

where

$$k_c = \left(\frac{t_c}{7}\right)^{b_c} \tag{18}$$

$$k_e = \left(\frac{1 - \left(\frac{RH}{100}\right)^5}{1 - \left(\frac{RH_{ref}}{100}\right)^5}\right)^{2.5} \quad \text{with } RH_{ref} = 65\ \% \tag{19}$$

$$W(t) = \left(\frac{t_0}{t}\right)^{\frac{\left(p_{SR} \cdot \frac{t_w}{365}\right)^{b_w}}{2}} \quad \text{with } t_0 = 0.0767 \text{ years} \tag{20}$$

In Eqs. (17)–(20), parameter k_c takes into account curing effects (the period of curing, t_c, and the exponent of regression, b_c, of the execution transfer parameter function k_c). Parameters k_e and C_S reflect the relative humidity (RH) and CO_2 concentration in the air, respectively. $R_{ACC,0}^{-1}$ is the inverse effective carbonation resistance of dry concrete, including the binding capacity of concrete for CO_2, determined at a certain time under accelerated carbonation conditions, k_t is a regression parameter and ε_t is an error term that considers the inaccuracies of the test method for accelerated carbonation conditions. The weather function, $W(t)$, which is dependent on time t, considers the influence of meso-climatic conditions (the rewetting of surfaces due to rain events) and ψ is the coefficient of model uncertainties. To express the weather function $W(t)$ according to the guidelines of *fib* Model Code 2010 (*fib* 2012), some other parameters are defined, i.e., the probability of driving rain, p_{SR}, time of wetness, t_w, (i.e., days with rainfall > 2.5 mm per day), and the exponent of regression of the weather function, b_w. The input random variables used in the presented example are listed in Table 1. Random variables are defined using the probability distribution function (PDF) of the random variable, μ is the mean value and CoV is the coefficient of variation. The mean value and variability of each variable were specified according to on-site measurements and recommendations of *fib* Bulletin No. 34 (*fib* 2006) and the JCSS.

In the context of the inputs the following should be added: the proper definition of some parameters might be problematic, e.g., the number of rainy days and the probability value of driving rain – both of them represent the age of the structure. Also, the estimation of the curing period is disputable in the case of such a cooling tower. These parameters were defined on the basis of experience with similar structures (e.g., Gehlen and Sodeikat 2002).

Table 2 presents a comparison of the analytical results based on Eq. (17) (noted as the *fib* model) with experimental data, namely the mean value μ and CoV of carbonation depth for both surfaces of the tower. The results obtained using the model extended by the correction factor (noted as the *fib* model with k_σ) are also mentioned. In this case, prevailing compressive stresses in the shell of the cooling tower caused by constant loading (dead load only) were assumed.

The rate of compressive stress and its ultimate value was assumed to be $\sigma_c/\sigma_{u,c}$ = 0.6. Hence, the correction factor value reaches 1.39 according to Eq. (8). It should be mentioned that the results were obtained based on probabilistic analysis. A thousand random realizations of input basic variables were simulated using the stratified

Table 1 Input parameters for modelling of concrete carbonation

Parameter	Unit	PDF	μ	CoV	Source
t	years	Deterministic	19.1	-	On-site measurements
C_S	mg/m^3	Normal	800	0.12	(Teplý *et al.* 2003)
RH external	%	Beta	70	0.07	*fib* Bulletin No. 34
RH internal	%	Beta	93	0.03	*fib* Bulletin No. 34
b_c	-	Normal	–0.567	0.04	*fib* Bulletin No. 34
t_c	days	Deterministic	1	-	(Gehlen and Sodeikat 2002)
$R_{ACC,0}^{-1}$	m^2/s/(kg/m^3)	Normal	9.8×10^{-11}	0.48	*fib* Bulletin No. 34
k_t	-	Normal	1.25	0.28	*fib* Bulletin No. 34
ε_t	m^2/s/(kg/m^3)	Normal	1×10^{-11}	0.15	*fib* Bulletin No. 34
t_w	days	Deterministic	27.3	-	(Gehlen and Sodeikat 2002)
p_{SR} external	-	Deterministic	0.2	-	(Gehlen and Sodeikat 2002)
p_{SR} internal	-	Deterministic	0.002	-	(Gehlen and Sodeikat 2002)
b_w	-	Normal	0.446	0.37	*fib* Bulletin No. 34
ψ	-	Lognormal	1	0.15	JCSS
$\sigma_c/\sigma_{u,c}$	-	Deterministic	0.6	-	Educated guess
a external	mm	Lognormal	28.4	0.30*	On-site measurements
a internal	mm	Lognormal	23.6	0.30*	On-site measurements

*On-site measurements; employed for reliability index assessment only

Latin Hypercube Sampling method implemented in FReET-D software. The calculations of carbonation depth x_c were performed repeatedly for an individual vector of realizations of input random variables and then statistically analyzed to obtain the mean value μ and the CoV of the carbonation depth (see Table 2). Considering the durability (the initiation period) of the analyzed structure, the limiting condition for the case of carbonation can be written using Eq. (9), which means that reinforcement depassivation and the consequent uniform corrosion of reinforcement can initiate at the time when the carbonation depth, x_c, permeates through the whole thickness of the concrete cover, *a*. Based on this assumption, the reliability level can be predicted over time. Black lines in Fig. 1 present the resulting reliability level for both surfaces of the analyzed cooling tower with the possible target reliability index of β_d = 1.3 according to *fib* Bulletin No. 34 (*fib* 2006).

As well as being able to predict the reliability level of a structure over time, we can follow the development of carbonation depth. This process is displayed using black lines in Figs. 2–3 for the external and internal surface of the cooling tower, respectively. In these figures the development of the mean carbonation depth value x_c over time can be seen for both of the analytical models used (the *fib* model and the extended *fib* model with k_σ, respectively) to reflect the coupled effects of mechanical and environmental loads. The dotted lines represent the standard deviation of carbonation depth over time.

An improvement is possible if the statistical information regarding behaviour gained by the analysis is combined with prior statistical information gained by measurements taken from a real structure at a certain age. For this purpose

Table 2 Carbonation depths x_c (in (mm)) in a cooling tower: Comparison of an analytical model with measurements on a real structure at the age of 19.1 years

	External surface		Internal surface	
	μ	CoV	μ	CoV
fib model	10.8	0.48	4.4	0.60
fib model with k_σ	15.0	0.48	6.1	0.57
On-site*	14.9	0.56	8.0	0.29

*On-site measurements (Keršner *et al.* 1996)

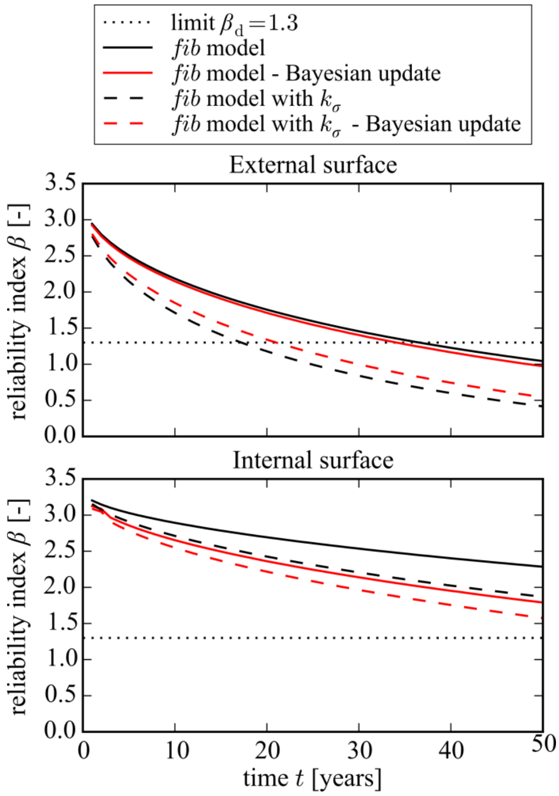

Fig. 1 Reliability profiles of a cooling tower

Bayesian updating was used (Ang and Tang 1975, Bažant and Chern 1984). On-site measurements of carbonation depth at the age of 19.1 years (see Table 2) were used to improve the estimations of carbonation depth over time as well as the reliability level of the cooling tower. The results are summarized using red lines in Figs. 1–3, and the variability of results obtained from mathematical modelling is lower. For this reason, the estimations of carbonation depth over time are more realistic using this procedure. Defining the service life t_S conservatively according to Eq. (4), it may be observed that the internal surface of the cooling tower meets the durability requirements for the whole design life t_D = 50 years. However, in the case of the external surface, the durability limit state is exceeded at 17 years according to the extended *fib* model with k_σ, (and at 21 years when utilizing the updating procedure). This corresponds in a reasonable extend with on-site measurements considering rather high variability of some input variables (e.g., according to on-site measurements the minimal value of concrete cover has been found 10 mm)

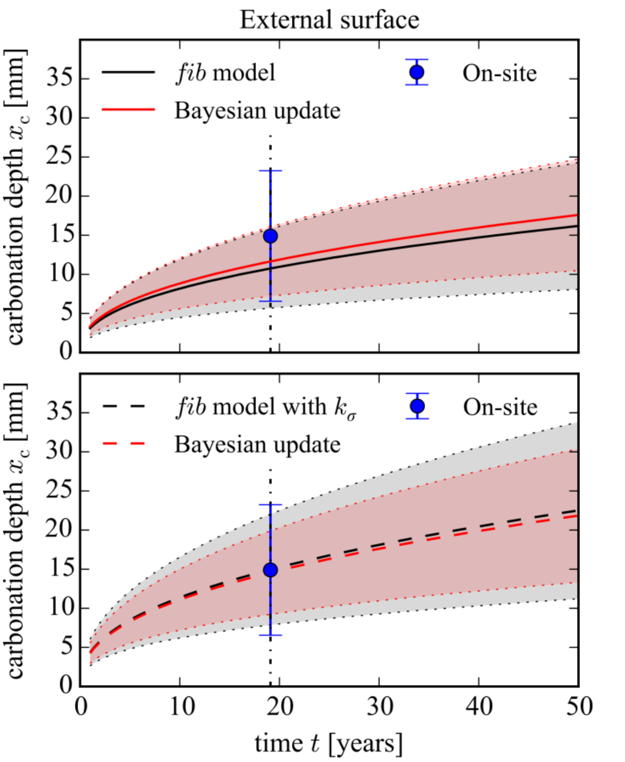

Fig. 2 Development of carbonation depth, x_c, in the external surface of a cooling tower over time

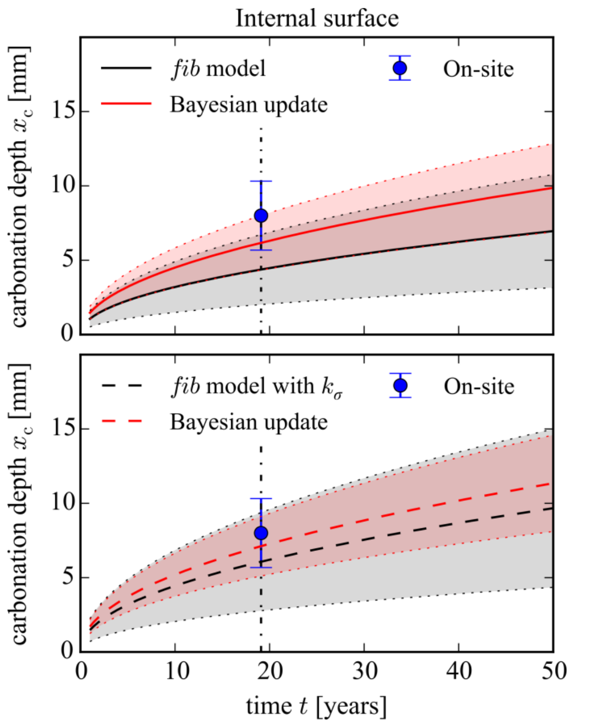

Fig. 3 Development of carbonation depth, x_c, in the internal surface of a cooling tower over time

and also the safety requirement $\beta \geq 1.3$. If the effect of actual stresses caused by mechanical loads were omitted, t_S would increase to about 35 years – such results can lead to incorrect (unsafe) decisions. Note that the modelled mean value for the internal surface is more “exact” than for the external one – most probably due to the almost steady humidity inside the tower and the marginal influence of rain.

In order to see the relative effect of each input parameter on the carbonation depth a sensitivity analysis was carried out. With respect to the Latin Hypercube Sampling simulation method utilized for reliability assessment, a non-parametric rank-order statistical correlation was performed by means of the Spearman correlation coefficient (Iman and Conover 1980). The method is based on the assumption that the random variable which influences the response variable (here the carbonation depth) most considerably (either in a positive or negative sense) will have a higher correlation coefficient than other variables. The results show that the relative humidity (*RH*) and the inverse effective carbonation resistance of dry concrete ($R_{ACC,0}{}^{-1}$) were the most dominant parameters in the case of internal surface assessment-their Spearman correlation coefficients were –0.7 and 0.45, respectively. Similar results were obtained based on the analysis of the dependence of input variables on the carbonation depth in the external surface. Here, the exponent of regression of the weather function (b_w) and again the inverse effective carbonation resistance of dry concrete ($R_{ACC,0}{}^{-1}$) affect the carbonation depth most-the correlation coefficients were 0.38 and 0.61, respectively.

In addition, the model uncertainty parameter (ψ) and regression parameter k_t have relatively high sensitivity (correlation coefficients of 0.38 and 0.36, respectively). The correlation coefficients for other parameters were less than 0.30.

5. Practical example for chloride ingress – a reinforced concrete beam

In this example the experimental measurements published by Francois and Arliguie (1999) are adopted in order to partially verify the practical usability of the model shown in section 3.3. Missing information from experimental measurements is supplied by nonlinear FEM calculations.

5.1 Experimental data

The experimental investigation published in (Francois and Arliguie 1999) studies the penetration of chlorides into reinforced concrete beams. The concrete mix was prepared using rounded gravel (silica and limestone), sand and Portland cement (OPC HP – high performance) with a water to cement ratio of 0.5. The average compression stress obtained on cylinder specimens was 45 MPa at 28 days. Two beams with the same geometry (see Fig. 4) were loaded in three point bending up to the moments of M_1 = 13.5 kNm (A1 beam) and M_2 = 21.2 kNm (A2 beam). Immediately after the loading occurred, the effects of both mechanical loading and a chloride environment began acting on the beams simultaneously and continued to do so for a time interval of 12 years.

Among other things, the penetration of free Cl^- ions into the middle of the beams was measured after 6 years of storage in a chloride environment at various depths from 5 to 65 mm. During this period the salt fog (35 g/l of NaCl)

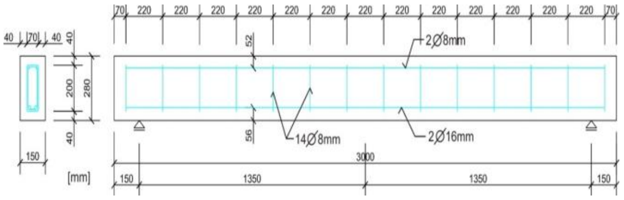

Fig. 4 The geometry of the tested reinforced concrete beam

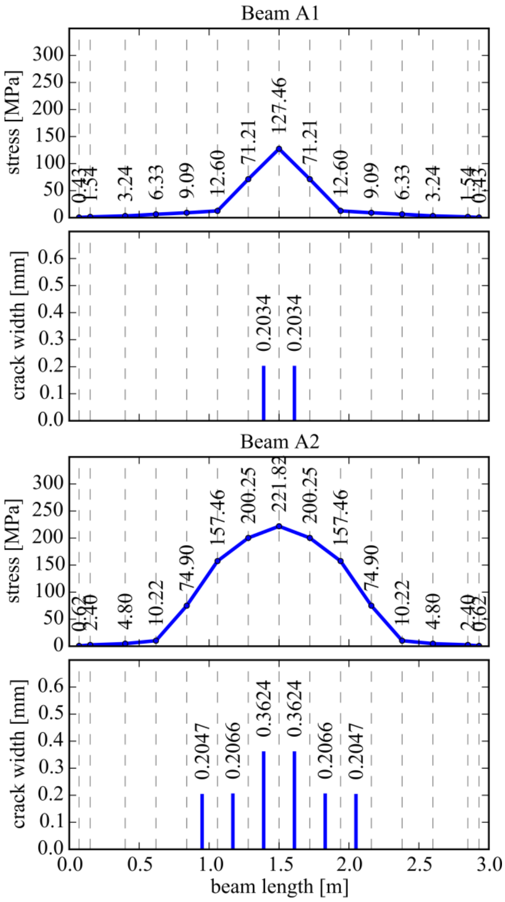

Fig. 5 Stresses in the reinforcement and crack widths on the tensioned surface of the beam loaded by moments M_1 and M_2 (corresponds to beams A1 and A2)

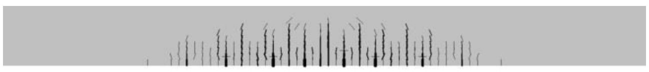

Fig. 6 Mapped crack pattern from the FEM analysis of beam A2 as an input layer for a CA simulation

was generated continuously and the storage temperature was 20℃.

5.2 Nonlinear FEM simulation of a beam in bending

The model of the beam was created in ATENA software in order to obtain the crack widths in tensioned parts of the beam loaded in three point bending. The so called "3D Non Linear Cementitious 2" model was used for the concrete, and the linear stress strain law was applied to the reinforcement. The beam geometry is presented in Fig. 4.

The loading produced bending moments of M_1 = 13.5 kNm (beam A1) and M_2 = 21.2625 kNm (beam A2)

Table 3 Input parameters for numerical simulations of chloride ion ingress into concrete

Parameter	Unit	PDF	μ	CoV	Source
x	mm	Deterministic	5–65		
Δx	mm	Deterministic	20 (A1); 5 (A2)		(Francois and Arliguie 1999)
t	years	Deterministic	6		(Francois and Arliguie 1999)
t_0	years	Deterministic	0.0767		
C_0	wt.-%/c	Deterministic	0		(Francois and Arliguie 1999)
$C_{S,\Delta x}$	wt.-%/c	Normal	0.05 (A1); 0.065 (A2)	0.40	(Francois and Arliguie 1999; Lollini *et al.* 2015)
$D_{app,C,ref}$	m^2/s	Normal	3.47×10^{-12}	0.20	(Francois and Arliguie 1999; Lollini *et al.* 2015)
w/c	-	Deterministic	0.5		(Francois and Arliguie 1999)
RH	%	Deterministic	100		(Francois and Arliguie 1999)
T	℃	Deterministic	20		(Francois and Arliguie 1999)
$s_{r,max}$	m	Normal	0.22	0.05	(Francois and Arliguie 1999)
w	mm	Deterministic	0.203408 (A1); 0.36245 (A2)		ATENA
F_ε	-	Deterministic	1.6		(Zhang *et al.* 2011)
F_c	-	Deterministic	1		(Zhang *et al.* 2011)
λ_e	-	Deterministic	0.27		(Zhang *et al.* 2011)

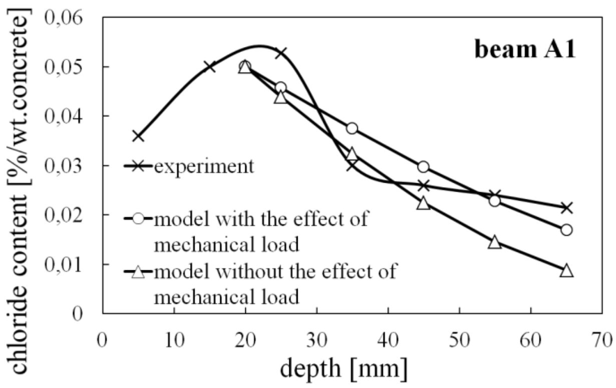

Fig. 7 Chloride content vs. depth (beam A1 after 6 years of exposure)

that correspond to the experimental setup. Moments M_1 and M_2 were used to calculate the tensile stresses in the reinforcement (Fig. 5). The resulting crack widths (see the simplified depiction in Fig. 5) served as the input parameters for the analytical calculations described in section 5.3. The more detailed crack pattern resulting from the FEM analysis of beam A2 is depicted in Fig. 6 and coincides well with experiment (Francois and Arliguie 1999).

5.3 Chloride ingress: numerical simulations and comparison to experimental data

Using the stochastic analytical model described in section 3.3, Eqs. (10) and (13), the ingress of free chloride ions into the middle of beams A1 and A2 was simulated and the results were compared to experimental measurements. The measured profiles of chloride concentration are depicted in Figs. 7–8. The chloride profile in the A1 beam indicates the presence of a convection zone (Fig. 7). This was numerically simulated by the authors of this paper and the results are described below.

The coefficients in Eq. (13) were specified in the following ways. In order to consider the influence of tensile or compressive stress states on $D_{\mathrm{app,C,ref}}$, correction coefficients were suggested according to Zhang *et al.* (2011): $F_\varepsilon = 1.6$ for a tensile state and 0.7 for a compressed stress state. Curing conditions were taken into account by using $F_\mathrm{c} = 1$ for a curing time of 7 days (Zhang *et al.* 2011). Environmental coefficient $F_\mathrm{e} = 1/\lambda_\mathrm{e}$, where $\lambda_\mathrm{e} = 0.27$ (Zhang *et al.* 2011) for a sea spray zone environment, which is the most similar environment to a salt fog of 35 g/l of NaCl (at a storage temperature of 20°C) was applied to the tested OPC concrete beams A1 and A2. F_w is given by Eq. (14). For F_T, F_h and F_t see Eqs. (21)–(22) (Zhang *et al.* 2011)

$$F_\mathrm{T} F_\mathrm{h} = \frac{\exp\left(14.2 - \dfrac{4210}{T}\right)}{1 + 256\left(1 - RH\right)^4} \tag{21}$$

$$F_\mathrm{t} = \left(\frac{t_0}{t}\right)^m \tag{22}$$

where T is the current temperature, RH is the relative humidity, t_0 is the reference or hydration time, t is the current time and m is the age factor. According to Zhang *et al.* (2011), m = 3(0.55-w/c) where w/c is the water to cement ratio. See Table 3 for the values and statistical characteristics of the input parameters used in the calculation (probabilistic distribution function PDF, mean value μ and coefficient of variation CoV). The depth of the convection zone Δx and the chloride content $C_{S,\Delta x}$ at depth Δx were estimated from the experimental results (depicted in Figs. 7–8).

In order to evaluate the benefit of considering the synergic effect of mechanical load and chloride ingress, a comparative calculation was also performed that did not include the effect of the load (w and F_ε were considered to be 0 mm and 1).

The results of the numerical simulation, and their comparison with experimental measurements, are given in Figs. 7–8 for beams A1 and A2, respectively. The amount of chloride ions at various depths in the centre of beams during the simultaneous action of loading and salt fog is shown.

It appears that the experimental and numerical results fit relatively well, thus verifying the model in certain respects as regards the synergy effect of mechanical and environmental loads (i.e., with consideration given to the current stress/strain state and the known width and spacing of cracks). Neglecting the effect of mechanical load leads to the undervaluation of the results to an unsafe degree. Unfortunately, the experimental findings (Francois and Arliguie 1999) do not provide chloride profiles for a non-loaded beam and for different boring positions.

The sensitivity analysis of input parameters that are considered to be random quantities was carried out by means of the Spearman correlation coefficient, as in the previous example. The results show that the most influential of them is the chloride content $C_{S,\Delta x}$ with its correlation coefficient of 0.99. The remaining parameters have sensitivities that are close to zero. The CoVs of the resulting chloride contents vary from 0.4 to about 0.42 for both the

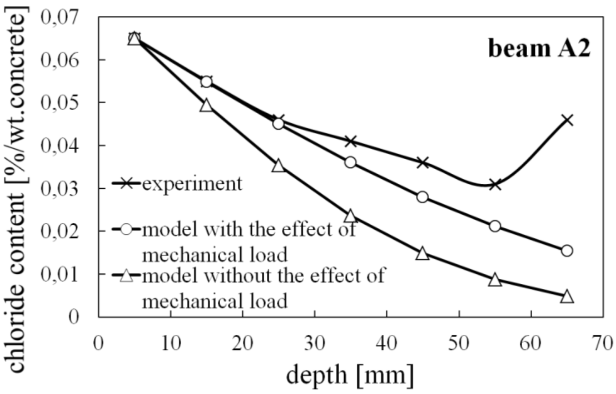

Fig. 8 Chloride content vs. depth (beam A2 after 6 years of exposure)

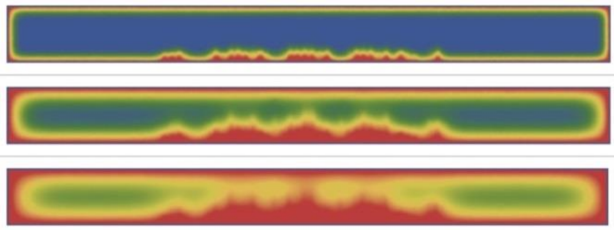

Fig. 9 Irregular spatial distribution of Cl^- concentrations after 6, 30 and 60 years of constant exposure for beam A2

A1 and the A2 beams. From the non-monotonic shape of the experimental curves it is evident that the existence of the effect of chloride ingress from all sides cannot be captured by the 1D solution utilized (where only the ingress in the vertical direction is modelled). Therefore, a 2D numerical approach based on the Cellular Automata (CA) technique has been employed as well, and is described in section 5.4.

5.4 Chloride ingress simulation using cellular automata

The CA solution to the diffusion process is based on the general formulation proposed by Biondini *et al.* (2004), Podroužek (2009) and further extended by implementing the directional effects due to local discontinuities (cracks) in the tested concrete specimens under mechanical loading. The inherent variability of such a process is reflected by the stochastic modification of the evolutionary coefficients (Vořechovská *et al.* 2009). In the case of isotropic media and a Von Neumann neighborhood scheme, the 4 adjacent cells will share an evolutionary coefficient of 0.125 and the central cell will have a value of 0.5 in order to satisfy the local normality rule. In the case of a local discontinuity, i.e., a crack with a specified dimension leading to accelerated diffusion, the isotropic evolutionary coefficient for this particular direction is increased by an equivalent of $F_\varepsilon = 1.6$, as used for the 1D analyses described above. The crack pattern (Fig. 6) is mapped to the CA array according to the resulting fracture process zone formation from the FEM analysis based on advanced material models (ATENA software). The resulting prognosis for the Cl^- concentration pattern is depicted in Fig. 9 considering the irregular spatial

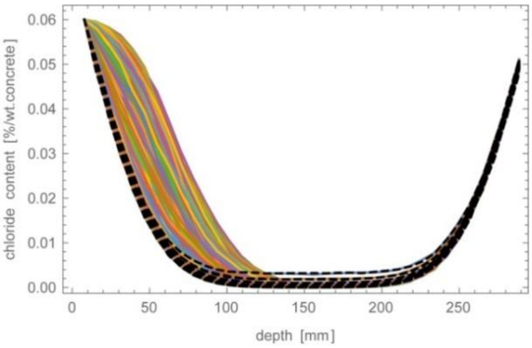

Fig. 10 Beam A2: scattering of simulated Cl^- profiles around the middle of the beam (transverse cut) at the reference period of 6 years

distribution of Cl^- concentrations after 6, 30 and 60 years of constant exposure for beam A2 (longitudinal cut in the loading plane at middle of the beam thickness).

The relationship between the cell size (C_x = 7 mm), time step duration length (Δt = 20 days), isotropic evolutionary coefficient (Φ_{iso} = 0.125) and diffusion coefficient ($D = 3.47\times10^{-12}$ m^2/s) is governed by the following rule

$$D = \Phi_{\text{iso}} C_x^2 \Delta t^{-1} \tag{23}$$

From here it follows that the directional effects attributed to the modification of Φ_{iso} can be physically interpreted as different diffusion coefficients applied locally. Furthermore, it can be stated that the region around the middle of the beam demonstrates large spatial variability in terms of both crack propagation and consequent chloride concentration. It is therefore difficult to compare experimental results represented by 1D Cl^- profiles (based on core samples extracted without considering the crack position) with analytical formulations if damaged (cracked) specimens are investigated.

Fig. 10 employs a transverse view to show the scatter of simulated Cl^- profiles around the middle of the beam A2 after the reference period of 6 years, where the strain reaches its maximum due to mechanical loading in bending. The scattering of simulated Cl^- profiles due to local discontinuities (cracks) is shown; the dashed line represents the reference case without discontinuities due to mechanical loading. Here note the uncertain characterization of a single point profile at lower depths (the region under tension) compared to the negligible scatter at the compression zone, where the transport process is not affected by cracking.

6. Conclusions

Cracking and changes in the pore structure in concrete are significant phenomena which need to be considered in service life modelling and while assessing the bearing capacity of concrete structures. These effects can accelerate deterioration process, resulting in reduced service life. To assess stress/strain fields and possible cracking, a nonlinear analysis of structural response can be performed using the finite element method based on fracture and damage mechanics.

This paper presents several models for analyzing the simultaneous effects of mechanical and environmental loads on concrete structures (namely the carbonation of concrete, and chloride ion diffusion) which are included in stochastic software with consideration given to inherent uncertainties.

It is believed that this allows an effective tool for the assessment and prediction of time-dependent degradation processes of concrete structures to be created, thus enabling the advanced modelling of the initial (and consequently the propagation) period. In this way the design and assessment of RC structures for durability are enhanced. 1D and 2D approaches are presented which enable at least a partial comparison with real structural behaviour, even in situations when there is a lack of comprehensive measurement data with a full description of structures loaded simultaneously by mechanical and environmental load over a significant time period.

The results reflect the coupled effects of mechanical and environmental loads on durability and the relevant reliability of reinforced concrete structures. An example of a cooling tower and a reinforced concrete beam loaded in three point flexion have been presented, showing the possibility of effectively modelling the influence of combined loads on service life and on structural reliability assessment. The possibility of enhancing the deterioration prognosis by utilizing real data for a certain age of a given structure via Bayesian updating is also shown with regard to the carbonation process at the cooling tower.

Results based on 1D modelling do not always sufficiently characterize the actual spatial variability of degradation processes, and the same is true of experimental measurements made on single point profiles only. On the other hand, the suggested simulation strategy based on a coupled FEM and CA approach provides unique quantitative feedback on uncertainty characterization in time and space.

Acknowledgments

This work has been supported by the project SPADD No. 14-10930S, awarded by the Grant agency of the Czech Republic (GACR), and project No. LO1408 “AdMaS UP-Advanced Materials, Structures and Technologies”, supported by the Ministry of Education of the Czech Republic under the “National Sustainability Programme I”. This support is gratefully acknowledged.

References

Andrade, C., Climent, M.A. and De Vera, G. (2015), “Procedure for calculating the chloride diffusion coefficient and surface concentration from a profile having a maximum beyond the concrete surface”, *Mater. Structs.*, **48**(4), 863-869.

Ang, A.H.S. and Tang, W.H. (1975), *Probability Concepts in Engineering Planning and Design, V. I, Basic Principles*, John Wiley and Sons, New York, U.S.A.

ATENA Software. http://www.cervenka.cz/.

Audenauert, K., De Schutter, G. and Marsavina, L. (2009), “Influence of cracks on chloride penetration and corrosion initiation time", *Proceedings of the 2nd International RILEM Workshop on Concrete Durability and Service Life Planning*, Haifa, Israel.

Bažant, Z.P. and Chern, J.C. (1984), "Bayesian statistical prediction of concrete creep and shrinkage", *ACI J*., **81**(4), 319-330.

Bentz, D.P., Garboczi, E.J., Lu, Y., Martys, N., Sakulich, A.R. and Weiss, W.J. (2013), "Modeling of the influence of transverse cracking on chloride penetration into concrete", *Cement Concrete Compos*., **38**, 65-74.

Beuhausen, H. (2014), "Pro 089: Principles of the performance-based approach for concrete durability", *Proceedings of the RILEM International Workshop on Performance-Based Specification and Control of Concrete Durability*.

Biondini, F., Bontempi, F., Frangopol, D.M. and Malerba, P.G. (2004), "Cellular automata approach to durability analysis of concrete structures in aggressive environments", *J. Struct. Eng*., **130**(11), 1724-1737.

Deung, C., Wang, S., Xiong, J., Fan, Z. and Xu, Y. (2013), "Influence of thickness deviation of concrete cover on durability design of concrete structures", *Proceedings of the 7th International Conference on Concrete under Severe Conditions-Environment and Loading*, Nanjing, China.

Djerbi, A., Bonnet, S., Khelidj, A. and Baroughel-Bouny, V. (2008), "Influence of transversing crack on chloride diffusion into concrete", *Cement Concrete Res*., **38**(6), 877-883.

EN 1992-1-1 (2004), *Eurocode 2: Design of Concrete Structures-Part 1-1: General Rules and Rules for Buildings*, European Committee for Standardization, Brussels, Belgium.

Fib (2006), *Fib Bulletin No. 34-Service Life Design*, Lausanne, Switzerland.

Fib (2012), *Fib Bulletins No. 65 & 66, Model Code 2010*, Lausanne, Switzerland.

Francois, R. and Arliguie, H. (1999), "Effect of microcracking and cracking on the development of corrosion in reinforced concrete members", *Mag. Concrete Res*., **51**(2), 143-150.

Fu, C., Jin, X., Ye, H. and Jin, N. (2015), "Theoretical and experimental investigation on loading effects on chloride diffusion in saturated concrete", *J. Adv. Concrete Technol*., **13**, 30-43.

Gehlen, C. and Sodeikat, C. (2002), "Maintenance planning of reinforced concrete structures: Redesign in a probabilistic environment inspection update and derived decision making", *Proceedings of the 9DBMC International Conference on Durability of Building Materials and Components*, Brisbane, Australia.

Iman, R.L. and Conover, W.J. (1980), "Small sample sensitivity analysis techniques for computer models with an application to risk assessment", *Commun. Stat. Theor. Meth*., **9**(17), 1749-1842.

Ishida, T., O'Neil Iqbal, P. and Anh, H.T.L. (2009), "Modeling of chloride diffusivity coupled with non-linear binding capacity in sound and cracked concrete", *Cement Concrete Res*., **39**(10), 913-923.

JCSS (2015), *Probabilistic Model Code-Part III*, Joint Committee on Structural Safety (JCSS), Denmark.

Jin, W.L., Yan, Y.D. and Wang, H.L. (2010), *Chloride Diffusion in the Cracked Concrete*, Fracture Mechanics of Concrete and Concrete Structures, Korea Concrete Institute, Seoul, Korea.

Keršner, Z., Novák, D., Teplý, B. and Bohdanecký, V. (1996), "Concrete carbonation, reinforcement corrosion and service life of a cooling tower", *Sanace*, **4**, 21-23.

Kim, D.G., Shimura, K. and Horiguchi, T. (2010), "Effect of tensile loading on chloride penetration of concrete mixed with granulated furnace slag", *J. Adv. Concrete Technol*., **8**(1), 27-34.

Leung, C.K.Y. and Hou, D. (2013), "Numerical simulation of chloride diffusion reinforced concrete structures with cracks", *Proceedings of the 7th International Conference on Concrete under Severe Conditions-Environment and Loading*, Nanjing, China.

Lollini, F., Carsana, M., Gastaldi, M., Radaelli, E. and Bertolini, L. (2015), "The challenge of the performance-based approach for the design of reinforced concrete structures in chloride bearing environment", *Constr. Build. Mater*., **79**, 245-254.

Lu, C.H., Gao, Y. and Liu, R.G. (2014), "Effect of transverse crack on chloride penetration into concrete subjected to drying-wetting cycles", *Proceedings of the 4th International Conference on Durability of Concrete Structures*, Purdue University, West Lafayette, Indiana, U.S.A.

Lu, Z., Zhao, Y., Yu, Z. and Ding, F. (2011), "Probabilistic evaluation of initiation time in RC bridge beams with load-induced cracks exposed to de-icing salts", *Cement Concrete Res*., **41**(3), 365-372.

Martín-Pérez, B., Zibara, H., Hooton, R.D. and Thomas, M.D.A. (2000), "A study of the effect of chloride binding on service life predictions", *Cement Concrete Res*., **30**(8), 1215-1223.

McKay, M.D., Conover, W.J. and Beckman, R.J. (1979), "A comparison of three methods for selecting values of input variables in the analysis of output from a computer code", *Technometr*., **21**, 239-245.

Miyazato, S. and Otsuki, N. (2010), "Steel corrosion induced by chloride or carbonation in mortar with bending cracks or joints", *Adv. Concrete Technol*., **8**(2), 135-144.

Mu, S., De Schutter, G. and Ma, B. (2013), "Non-steady state chloride diffusion in concrete with different crack densities", *Mater. Structs*., **46**, 123-133.

Novák, D., Vořechovský, M. and Teplý, B. (2014), "FReET-software for the statistical and reliability analysis of engineering problems and FReET-D: Degradation module", *Adv. Eng. Softw*., **72**, 179-192.

Oh, B.H. and Jang, S.Y. (2007), "Effects of material and environmental parameters on chloride penetration profiles in concrete structures", *Cement Concrete Res*., **37**(1), 47-53.

Papakonstantinou, K.G. and Shinozuka, M. (2013), "Probabilistic model for steel corrosion in reinforced concrete structures of large dimensions considering crack effects", *Eng. Struct*., **57**, 306-326.

Podroužek, J. (2009), "Stochastic cellular automata in dynamic environmental modelling: Practical applications", *Electr. Not. Theor. Comput. Sci*., **252**, 143-156.

Podroužek, J., Bucher, C. and Deodatis, G. (2014), "Identification of critical samples of stochastic processes towards feasible structural reliability applications", *Struct. Saf*., **47**, 39-47.

Podroužek, J., Strauss, A. and Novák, D. (2015), "Spatial degradation in reliability assessment of ageing concrete structures", *Proceedings of the 1st International Conference on Uncertainty Quantification in Computational Sciences and Engineering*, Crete, Greece.

RILEM (2013), P*ublications on Durability of Reinforced Concrete Structures under Combined Mechanical Loads and Environmental Actions: An Annotated Bibliography*, Report rep043.

Schneider, R., Fischer, J., Bügler, M., Nowak, M., Thöns, S., Borrmann, A. and Straub, D. (2015), "Assessing and updating the reliability of concrete bridges subjected to spatial deterioration-principles and software implementation", *Struct. Concrete*, **16**(3), 356-365.

Tang, S.W., Yao, Y., Andrade, C. and Li, Z.J. (2015), "Recent durability studies on concrete structures", *Cement Concrete Res*., **78**, 143-154.

Teplý, B., Chromá, M., Rovnaník, P. and Novák, D. (2012), "Role of modelling in probabilistic durability assessment of concrete structures", *Proceedings of the 3rd International Symposium on*

Life-Cycle and Sustainability of Civil Infrastructure Systems, Vienna, Austria.

Teplý, B., Králová, H., Stewart, M.G. (2003), "Ambient carbon dioxide, carbonation and deterioration of RC structures", *J. Mater. Struct. Reliab.*, **1**, 31-36.

Vanmarcke, E., Shinozuka, M., Nakagiri, S., Schueller, G.I. and Grigoriu, M. (1986), "Random fields and stochastic finite elements", *Struct. Saf.*, **3**(3-4), 143-166.

Vořechovská, D., Podroužek, J., Chromá, M., Rovnaníková, P. and Teplý, B. (2009), "Modelling of chloride concentration effect on reinforcement corrosion", *Comput. Aid. Civil Infrastruct. Eng.*, **24**(6), 446-458.

Wan, X., Wittmann, F.H., Zhao, T. and Jiang, F. (2013), "Chloride penetration into concrete after uniaxial compression", *J. Front. Constr. Eng.*, **2**(3), 66-74.

Wang, L. and Ueda, T. (2011), "Mesoscale modelling of the chloride diffusion in cracks and cracked concrete", *J. Advs Concrete Technol.*, **9**(3), 241-249.

Wittmann, F.H., Jiang, F., Zhao, T., Wan, X. and Zhang, P. (2012), "Durability of concrete and service life of reinforced concrete structures under combined mechanical and environmental actions", *Proceedings of the 7th Annual Concrete Conference*, Qingdao, China.

Yuan, Q., Shi, C., De Schutter, G., Audenaurt, K. and Deng, D. (2009), "Chloride binding of cement-based materials subjected to external chloride environment-a review", *Constr. Build. Mater.*, **23**(1), 1-13.

Zhang, X., Zhao, Y., Xing, F. and Lu, Z. (2011), "Coupling effects of influence factors on probability of corrosion initiation time of reinforced concrete", *J. Centr. South Univ. Technol.*, **18**(1), 223-229.

CC